Controlled Synthesis and Transfer of Large-Area WS_2 Sheets: From Single Layer to Few Layers

Ana Laura Elías,[†] Néstor Perea-López,[†] Andrés Castro-Beltrán,[†,‡] Ayse Berkdemir,[†] Ruitao Lv,[†] Simin Feng,[†] Aaron D. Long,[†] Takuya Hayashi,[§] Yoong Ahm Kim,[§] Morinobu Endo,[§] Humberto R. Gutiérrez,[⊥] Nihar R. Pradhan,[∥] Luis Balicas,[∥] Thomas E. Mallouk,[†,#] Florentino López-Urías,[†,△] Humberto Terrones,[†] and Mauricio Terrones[†,#,□,▽,*]

[†]Department of Physics and Center for 2-Dimensional and Layered Materials, The Pennsylvania State University, University Park, Pennsylvania 16802, United States , [‡]Facultad de Ingeniería Mecánica y Eléctrica (FIME), Universidad Autónoma de Nuevo León, Avenida Universidad s/n Ciudad Universitaria, San Nicolás de los Garza, NL 66450, México, [§]Faculty of Engineering, Shinshu University, 4-17-1 Wakasato, Nagano, 380-8553, Japan, [⊥]Department of Physics & Astronomy 102, Natural Science Building, University of Louisville, Louisville, Kentucky 40292, United States, [∥]National High Magnetic Field Laboratory, Florida State University, Tallahassee, Florida 32310, United States, [#]Department of Chemistry, The Pennsylvania State University, University Park, Pennsylvania 16802, United States, [△]Advanced Materials Department, IPICyT, San Luis Potosí, SLP 78216, México, [□]Department of Materials Science and Engineering & Materials Research Institute, The Pennsylvania State University, University Park, Pennsylvania 16802, United States, and [▽]Research Center for Exotic Nanocarbons (JST), Shinshu University, Wakasato 4-17-1, Nagano, 380-8553, Japan

ABSTRACT The isolation of few-layered transition metal dichalcogenides has mainly been performed by mechanical and chemical exfoliation with very low yields. In this account, a controlled thermal reduction—sulfurization method is used to synthesize large-area (~1 cm^2) WS_2 sheets with thicknesses ranging from monolayers to a few layers. During synthesis, WO_x thin films are first deposited on Si/SiO_2 substrates, which are then sulfurized (under vacuum) at high temperatures (750—950 °C). An efficient route to transfer the synthesized WS_2 films onto different substrates such as quartz and transmission electron microscopy (TEM) grids has been satisfactorily developed using concentrated HF. Samples with different thicknesses have been analyzed by Raman spectroscopy and TEM, and their photoluminescence properties have been evaluated. We demonstrated the presence of single-, bi-, and few-layered WS_2 on as-grown samples. It is well known that the electronic structure of these materials is very sensitive to the number of layers, ranging from indirect band gap semiconductor in the bulk phase to direct band gap semiconductor in monolayers. This method has also proved successful in the synthesis of heterogeneous systems of MoS_2 and WS_2 layers, thus shedding light on the controlled production of heterolayered devices from transition metal chalcogenides.

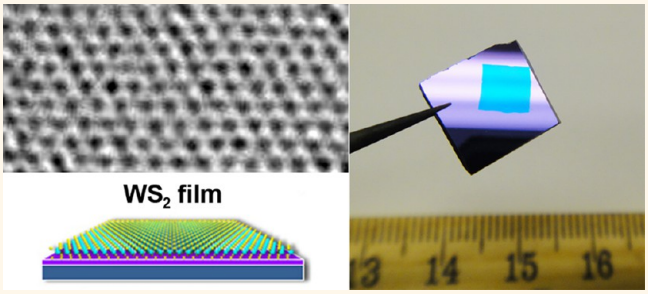

KEYWORDS: synthesis · WS_2 · chalcogenides · single layers · characterization · optical properties

Transition metal dichalcogenides (MoS_2, WS_2, WSe_2, $MoSe_2$, NbS_2, $NbSe_2$, *etc.*) are layered materials that can exhibit semiconducting, metallic and even superconducting behavior. In the bulk form, the semiconducting phases (MoS_2, WS_2, WSe_2, $MoSe_2$) have an indirect band gap. Recently, these layered systems have attracted a great deal of attention[1−12] mainly due to their complementary electronic properties when compared to other two-dimensional materials, such as graphene (a semimetal)[13] and boron nitride (an insulator).[14,15] However, these bulk properties could be significantly modified when the system becomes monolayered; the indirect band gap becomes direct. Such changes in the band structure when reducing the thickness of a WS_2 film have important implications for the development of novel applications, such as valleytronics.[16,17]

In particular, the layered structure of metal chalcogenides is formed by the stacking of three atomic layers of sulfur—metal—sulfur. For WS_2, the crystal belongs to the $P6_3/mmc$ space group ($a = 3.155, c = 12.36$),[18]

* Address correspondence to mut11@psu.edu.

Received for review February 25, 2013 and accepted May 6, 2013.

Published online May 06, 2013
10.1021/nn400971k

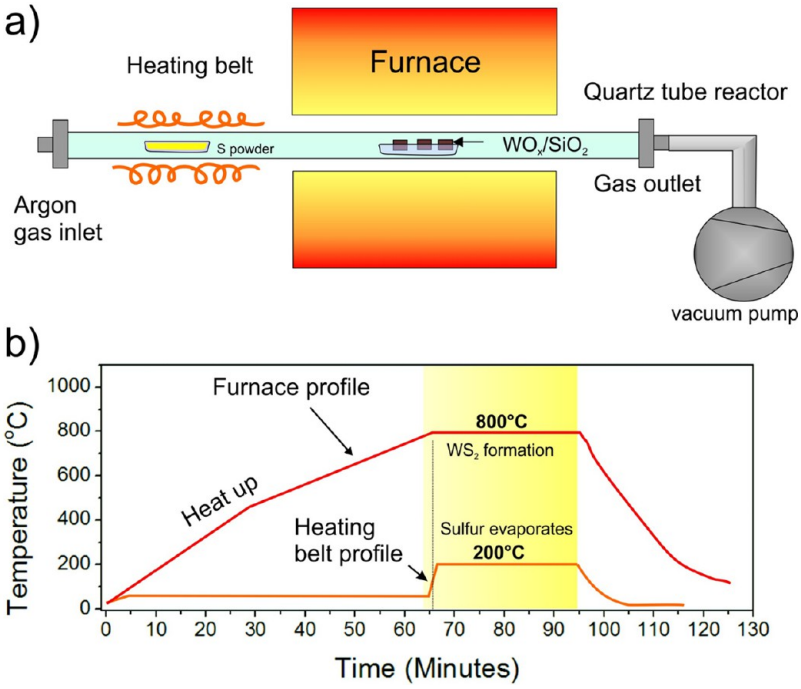

Figure 1. (a) Schematic representation of the experimental setup used for the synthesis of WS_2 films involving high-temperature treatments under a sulfur/argon environment at low pressures (450 mTorr). (b) Temperature ramp used for the sulfurization experiments.

and its planar projection shows a perfect hexagonal lattice of S atoms, with interleaved W atoms coordinated by S in a trigonal prismatic arrangement. The structure is similar to that of MoS_2 and some of the other dichalcogenides.

Significant attempts have been made to isolate/grow monolayers of WS_2 and MoS_2 by different routes, these being mainly mechanical and chemical exfoliation.[2,3,6,7,10,19] More recently, chemical vapor deposition (CVD) routes have been used in order to synthesize few-layered MoS_2 sheets.[4,20−22] A microwave-assisted method has also been developed in order to prepare few-layered nanoflakes of MoS_2 and WS_2 and other metal dichacogenides.[23] The isolation of few-layered WS_2 and MoS_2 has allowed researchers to better understand their physicochemical properties including transport,[24] photocurrent,[25] photoluminescence,[1,3,5,6] stiffness,[26] magnetism,[23] and valley polarization.[16,17] In addition, striking photoluminescence (PL) and PL edge enhancement properties have been measured in triangular monolayered WS_2 clusters.[1] Although monolayered triangular islands of WS_2[1] and MoS_2[20−22] have been recently reported using CVD techniques, to the best of our knowledge, the controlled growth of large-area monolayered WS_2 has not been reported hitherto. More recently, double-resonance Raman has demonstrated that it is now possible to clearly identify and distinguish monolayered WS_2 when a 514.5 nm laser excitation wavelength is used; the Raman spectra are different when comparing monolayers with few layered and bulk WS_2.[27] Such advances stimulate further attempts to synthesize and also to characterize the physical properties of large-area monolayers of WS_2. These monolayers could also be mixed with graphene and/or hexagonal boron nitride in order to produce novel heterolayered materials with unprecedented properties.

In this work, we report for the first time the controlled synthesis of large-area (~cm^2) single-, bi-, and few-layer WS_2 using a two-step process (see Figure 1 for details). WO_x thin films were deposited onto a Si/SiO_2 substrate, and these films were then sulfurized under vacuum in a second step occurring at high temperatures (750−950 °C). Furthermore, we have developed an efficient route to transfer these WS_2 films onto different substrates, such as quartz and TEM grids, using concentrated HF (see Figure 2 for details). WS_2 films of different thicknesses have been analyzed by optical microscopy, Raman spectroscopy, and high-resolution transmission electron microscopy (HRTEM). The photoluminescence properties of these films are also discussed below.

RESULTS AND DISCUSSION

Raman spectroscopy on both as-grown and transferred WS_2 films was performed in a Renishaw inVia confocal microscope-based Raman spectrometer using the 488 and 514.5 nm laser excitations. The 520.5 cm^{-1} phonon mode from the Si substrate was used for calibration. Raman spectroscopy has become an essential tool for studying two-dimensional single layers of different layered materials such as graphene,[28−30]

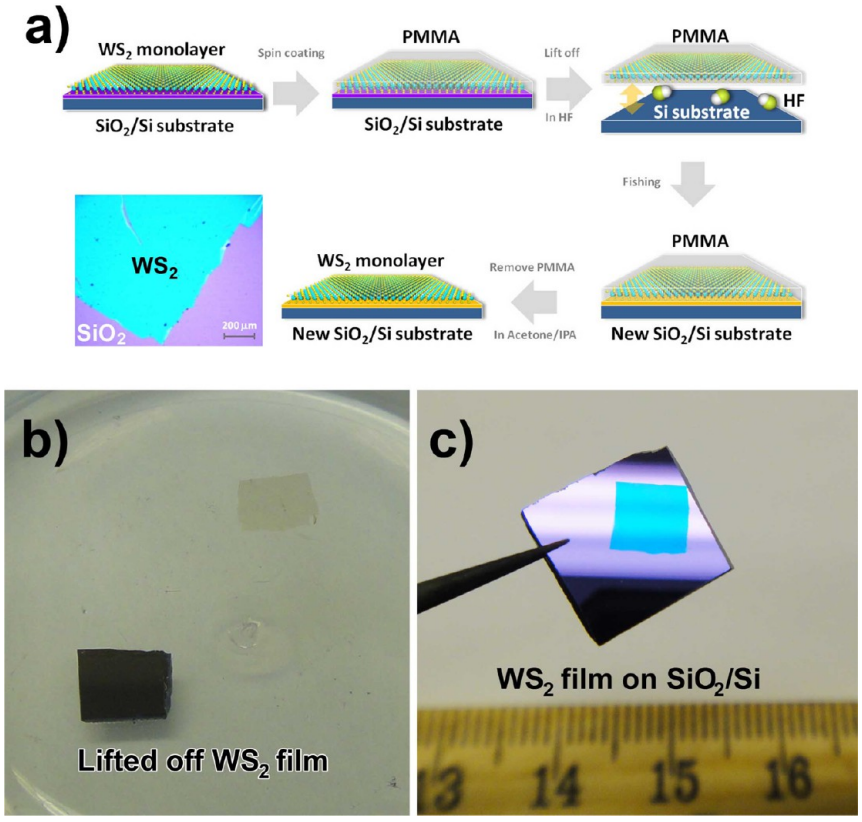

Figure 2. (a) Schematic representation of the polymethyl methacrylate (PMMA)-assisted transfer method onto different substrates. (b) Photograph of the WS_2 film floating on hydrofluoric acid (HF). (c) Photograph of a WS_2 film on a SiO_2/Si substrate, exhibiting the high contrast and color change (films appear in a cyan color upon contrast with the SiO_2 substrate).

BN,[31] and transition metal dichalcogenides.[1,27,32−35] For MoS_2 and WS_2, the first-order Raman spectra in the backscattering geometry show two optical phonon modes [$E^1_{2g}(\Gamma)$ and $A_{1g}(\Gamma)$] and one longitudinal acoustic mode [LA(M)]. Inset cartoons in Figure 3b show the directions of the atomic vibrations for the $E^1_{2g}(\Gamma)$ and $A_{1g}(\Gamma)$ modes; $E^1_{2g}(\Gamma)$ is an in-plane optical mode, while $A_{1g}(\Gamma)$ corresponds to out-of-plane vibrations of the sulfur atoms. The frequencies of these modes for bulk have been well determined in the past by using both Raman[36,37] and neutron scattering.[38] $E^1_{2g}(\Gamma)$, $A_{1g}(\Gamma)$, and LA(M) modes for bulk WS_2 (MoS_2) appear at around 356 cm^{-1} (382 cm^{-1}), 421 cm^{-1} (408 cm^{-1}), and 176 cm^{-1} (226 cm^{-1}), respectively. For few layers, these frequencies undergo small variations due to the decreasing interlayer interactions, and these variations can be used to determine the presence of single-layer films.[1,27,32,33] Additional peaks in the WS_2 spectrum correspond to multiphonon combinations of these primary modes. In the present study, the WS_2 spectra obtained in all samples match previous Raman studies.[27,36] Few- and single-layer WS_2 films were identified by monitoring both the relative intensities and the spectral positions of the 2LA(M), E^1_{2g}, and A_{1g} phonon modes.[27] Typical single-layered WS_2 Raman spectra acquired using 488 and 514.5 nm excitation wavelengths are shown in Figure 3. When using a 514.5 nm laser line, the A_{1g} mode was identified at *ca.* 418.3 cm^{-1}; the E^1_{2g} mode at *ca.* 356 cm^{-1} was overshadowed by the presence of the high-intensity 2LA(M) phonon mode located at 353 cm^{-1}. As stated in the introduction and according to previously reported theoretical and experimental data,[27] a double-resonance Raman process occurs for single-layered WS_2 that causes the 2LA(M) to emerge with an intensity much larger (double) than that of the A_{1g} mode, as shown in Figure 3a. This effect can be used to easily identify single-layer WS_2 when using the 514.5 nm laser excitation wavelength.[27] When using the 488 nm laser excitation wavelength, the more intense Raman peaks are the $E^1_{2g}(\Gamma)$ and $A_{1g}(\Gamma)$, while the intensities of the second-order Raman peaks are weaker when compared to those observed for the 514.5 nm excitation wavelength (see Figure 3b). The 2LA(M) resonance is also absent for λ_{exc} = 488 nm. Raman mappings of monolayered WS_2 films were acquired using the 514.5 nm laser line in order to demonstrate the uniformity of our samples (see Figure 3c and d). It is noteworthy that the 2LA(M) phonon mode is constantly much more intense when compared to the A_{1g} mode, and that provides evidence of the uniformity of our WS_2 monolayers. Raman spectra were acquired from samples in their original substrate and also after transfer onto clean Si/SiO_2 substrates, showing no variations.

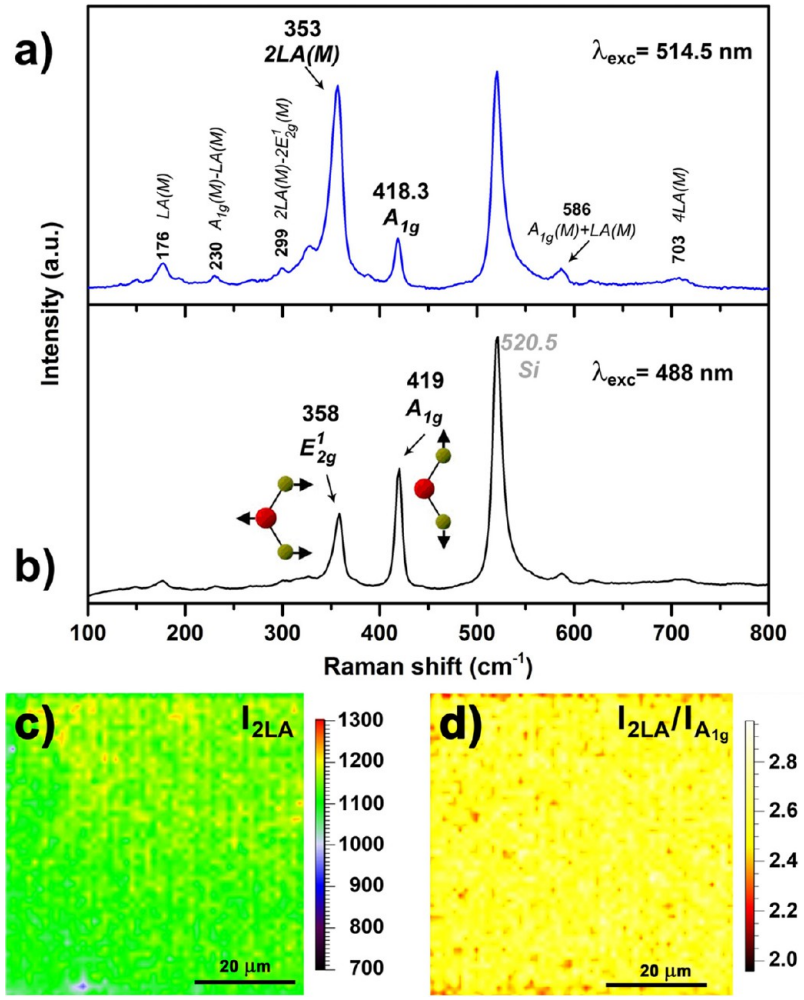

Figure 3. Raman characterization of monolayered WS_2 films with different excitation wavelengths: (a) 514.5 nm and (b) 488 nm. (c) 2LA(M) intensity map. (d) Intensity ratio map of 2LA(M) over A_{1g}, which provides information of the uniformity of the monolayer of WS_2. All Raman spectra were acquired from samples synthesized with the thinnest (1 nm) prepared WO_x film.

HRTEM characterization was performed on WS_2 samples transferred onto Quantifoil gold TEM grids with 2 μm holes. A JEOL JEM-2100F microscope equipped with double Cs-correctors, operated at 120 and 80 kV, was used. Image acquisition and processing (FFT, IFFT, *etc.*) were performed using the Gatan Digital Micrograph software. Figure 4a exhibits the WS_2 hexagonal lattice. Although the sample has a fairly high crystalline quality, a few defects can be observed in Figure 4a. Further investigations on the local electronic states of these defects are needed in order to find if they act as p-type or n-type dopants, or as traps for free carriers. During the transfer process, WS_2 films could be folded or wrinkled; due to this fact, we could also find some regions with different WS_2 thickness and stacking. Figure 4b and c exhibit both bilayer and trilayer WS_2 with different stacking order, indicated by the presence of Moiré patterns and confirmed by the respective fast Fourier transforms (see insets). Figure 4d depicts the edge of a single-layered WS_2 film synthesized through the sulfurization of a 1 nm thick WO_x film. 2L and 3L films can be obtained by sulfurizing 2 and 2.8 nm thick oxide films, respectively.

In order to study photoluminescence, WS_2 samples were illuminated with a 488 nm excitation wavelength (Figure 5a and b). Recently, PL signals have been experimentally observed in monolayered WS_2 and MoS_2,[1,3,5,6] and our monolayered WS_2 films exhibit PL. The bulk phase of WS_2 possesses an indirect electronic band gap of around 1.4 eV and a direct band gap of 2.01 eV,[9] whereas single-layered WS_2 exhibits a direct band gap at *ca.* 1.9 eV, in close agreement with DFT-LDA calculations.[36,39−41] Figure 5c and d display the calculated electronic band structure for both monolayered and bulk WS_2. Therefore, a PL signal located at around 1.9 eV indicates the presence of single-layered WS_2. Experimental PL spectra are shown in Figure 5a, where single-layered WS_2 shows a relatively sharp PL peak centered at *ca.* 2.02 eV (613 nm). A very weak PL signal was found for double-layered WS_2 samples at *ca.* 1.93 eV (642 nm), with a shoulder located at 2.17 eV (571 nm). For trilayered samples, an extremely weak PL signal was found at 1.92 eV (647 nm) and a weaker signal was found at 2.18 eV (570 nm). PL maps of 60 × 60 μm regions were carried

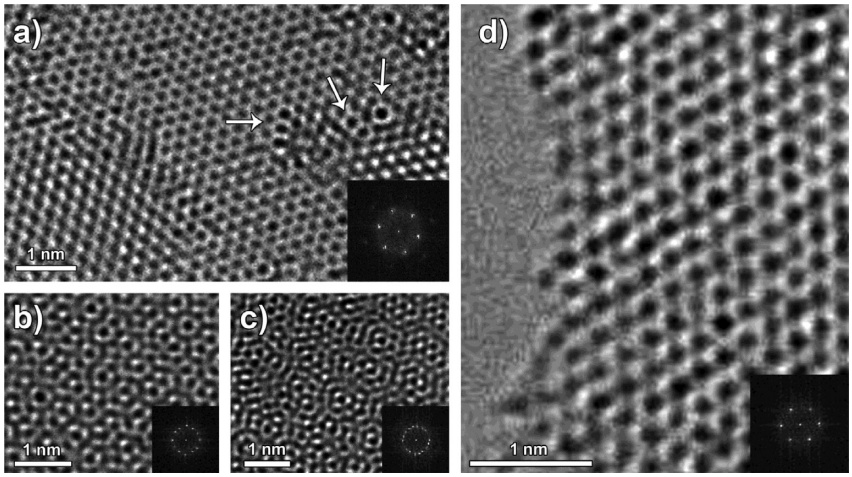

Figure 4. HRTEM images of WS_2 films. Insets show the fast Fourier transformation (FFT) of the corresponding TEM micrograph. (a) WS_2 film exhibiting crystalline regions and some defects, such as larger rings, highlighted by arrows. (b and c) Bilayer and trilayer WS_2 with different stacking, revealed by the formed Moiré pattern and confirmed by the FFT. (d) Edge of a single-layer WS_2 film.

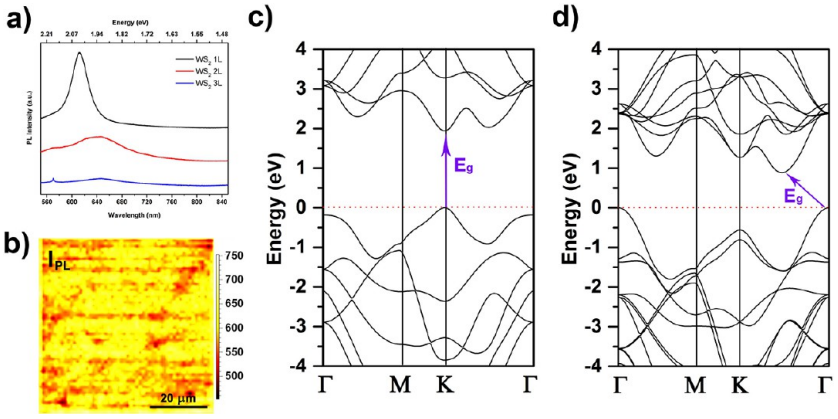

Figure 5. (a) Photoluminescence (PL) spectra of single-, bi-, and trilayer WS_2 films. (b) PL intensity map, exhibiting the uniform signal collected from our films. The map was acquired using a 1.1 μm step size. (c) Band structure of single-layer WS_2. (d) Band structure of bulk WS_2.

out in single-layered WS_2 samples to show their uniformity (see Figure 5b).

The synthetic method described above is very versatile. High-quality few-layered WS_2 and MoS_2 were also obtained following this method, but at atmospheric pressure. For these experiments, an Ar flow of 100 sccm was used, while the rest of the setup remains as described in Figure 1. Interestingly, hybrid systems (MoS_2−WS_2) can also be synthesized by adding an extra layer of MoO_x onto the $Si/SiO_2/WO_x$ substrates. By using 2 nm WO_x and 2 nm MoO_x, a few-layer hybrid material, so-called $W_xMo_yS_2$, has been identified by Raman spectroscopy (see Figure 6). The spectrum exhibits the strongest bands corresponding to both MoS_2 and WS_2 (E^1_{2g} and A_{1g}). In Figure 6a, those bands are highlighted in green for WS_2 (352.2 and 418 cm^{-1}) and in red for MoS_2 (381 and 408.3 cm^{-1}). In this context, hybrid $W_xMo_{1-x}S_2$ single layers have been recently isolated by mechanical exfoliation of chemical vapor transport grown crystals.[42] W and Mo were visualized by scanning transmission electron microscopy.[42] Interestingly, a theoretical report has also appeared in the literature, providing more evidence of the feasibility of $W_xMo_yS_2$ and other in-plane hybrid structures, such as $MoS_2/MoSe_2$.[43] For the $W_xMo_yS_2$ synthesized by us, Raman spectroscopy suggests that both WS_2 and MoS_2 coexist within the same material. Raman mappings have been performed using a 514.5 nm excitation wavelength (see Figure 6a−d). Raman mappings shown in Figure 6b and c depict the intensity of the E^1_{2g} phonon mode associated with MoS_2 and WS_2, respectively. Regions of higher and lower intensities were captured in these maps. In order to better present the intensity differences between both signals, a ratio intensity map of WS_2 E^1_{2g} over MoS_2 E^1_{2g} is shown in Figure 6d. The brighter regions correspond to WS_2 richer regions. This could be an indication of crystalline domains in an in-plane blended film. Our method sheds light on the production of heterogeneous transition metal chalcogenide structures, and electron

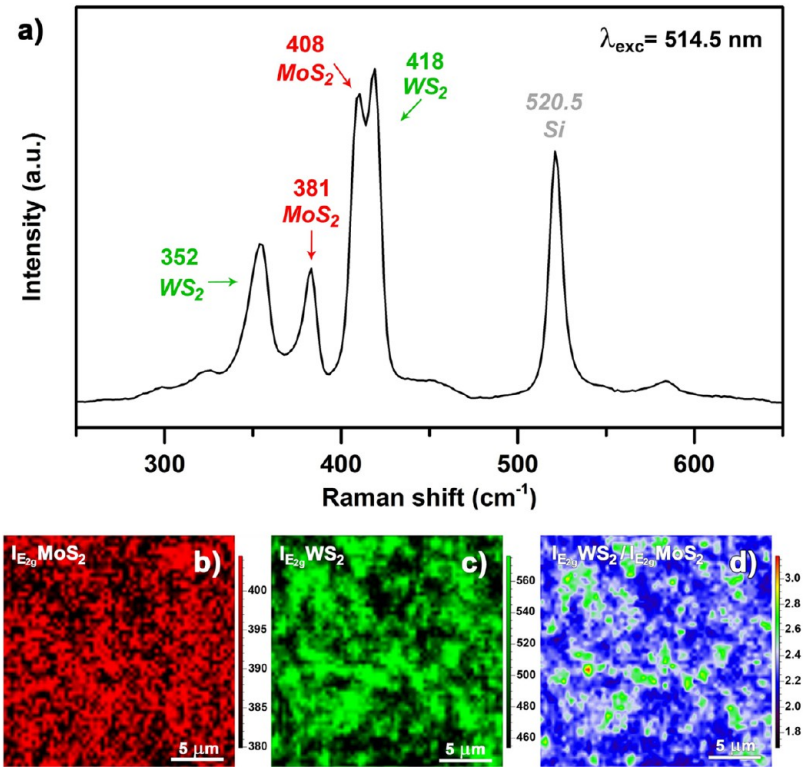

Figure 6. (a) Raman spectrum of a hybrid MoS_2–WS_2 film grown directly on Si/SiO_2 at atmospheric pressure. (b) E^1_{2g} intensity map associated with MoS_2. (c) E^1_{2g} intensity map associated with WS_2. (d) Intensity ratio map of WS_2 E^1_{2g} over MoS_2 E^1_{2g}. All the spectra were acquired with a 514.5 nm laser excitation wavelength.

microscopy investigations are currently being performed in order to clearly assess the nature of this new hybrid material.

CONCLUSIONS

WS_2 films were produced by a thermal reduction–sulfurization method achieving large-area sheets ($\sim cm^2$) and controllable thicknesses ranging from one to several layers. The WS_2 sheets were characterized by optical microscopy, Raman spectroscopy, HRTEM, and optical spectroscopy. From HRTEM characterization and further analysis by fast Fourier transform (FFT), we determined the different WS_2 thicknesses. Bilayer and trilayer WS_2 with different layer stackings were confirmed by the formation of Moiré patterns and FFT. WS_2 samples were targeted with a 488 nm excitation wavelength in order to analyze PL spectra, and we observed that only single-layer WS_2 gave a prominent PL signal located at around 2.0 eV. Investigations related to applications of monolayered WS_2-based photosensor devices and gas sensing are currently under way. This thermal sulfurization method of synthesizing large-area WS_2 could now be implemented for the synthesis of other dichalcogenide materials such as MoS_2, $MoSe_2$, WSe_2, NbS_2, and $NbSe_2$. For instance, the method has been used to successfully produce few-layered hybrid $W_xMo_yS_2$ materials, as confirmed by Raman spectroscopy.

EXPERIMENTAL DETAILS

Si wafers with a thermally deposited 285 nm thick SiO_2 layer were cleaned with acetone–2-propanol mixtures in an ultrasonic bath for 15 min. After drying with compressed ultra-high-purity (UHP) N_2 gas, the wafers were loaded in the chamber of a physical vapor deposition apparatus, PVD75 (Kurt J. Lesker). WO_3 was thermally evaporated and deposited on the wafers; various thicknesses ranging from 1 to 18 nm were deposited at low pressures (10^{-5}–10^{-6} Torr). For the hybrid $W_xMo_yS_2$, MoO_3 was thermally evaporated onto a WO_x-coated substrate. Si wafers were subsequently loaded into a quartz reaction tube (35 mm i.d. × 38 mm) for thermal treatment under a sulfur environment, as shown in Figure 1. A boat with 500 mg of S powder (99.5%, Alfa Aesar, CAS 7704-34-9) was placed outside the furnace; this zone was wrapped with a heating belt, which was heated to a temperature of 200 °C. The pressure in the chamber was reduced to 35 mTorr for 10 min, and UHP Ar (50 sccm) was then allowed to flow into the reaction tube, reaching a pressure of 450 mTorr. The split furnace was then heated to temperatures ranging from 750 to 900 °C. Typical temperature ramps for both the furnace and the heating belt are shown in Figure 1b.

The chemical method developed for the transfer of as-grown WS_2 films is shown in Figure 2a. WS_2 films were covered with a thin layer of poly(methyl methacrylate) by spin coating at 4000 rpm for 60 s (MW 495 000, A3). After a 2 h polymer curing step, samples were immersed in hydrofluoric acid (ACS, 48–51%, Alfa Aesar, CAS 7664-39-3) for a few seconds in order to lift off the PMMA–WS_2 material. The films were then fished out with Mo foil and immersed in deionized water. Finally, the

films were fished out with the desired substrate (quartz, TEM grids, *etc.*) and allowed to dry under ambient conditions. In order to remove the PMMA coating, the samples were washed in acetone and 2-propanol.

Conflict of Interest: The authors declare no competing financial interest.

Acknowledgment. This work is supported by the U.S. Army Research Office MURI grant W911NF-11-1-0362, the Materials Simulation Center of the Materials Research Institute, the Research Computing and Cyberinfrastructure unit of Information Technology Services, and Penn State Center for Nanoscale Science. M.T. thanks JST-Japan for funding the Research Center for Exotic NanoCarbons, under the Japanese regional Innovation Strategy Program by the Excellence. M.T. and T.E.M. also acknowledge support from the Penn State Center for Nanoscale Science for a seed grant on 2-D Layered Materials (DMR-0820404). The authors also acknowledge the Center for 2-Dimensional and Layered Materials. The authors are grateful to Zhong Lin and Lakshmy Pulickal Rajukumar for technical assistance.

REFERENCES AND NOTES

1. Gutiérrez, H. R.; Perea-López, N.; Elías, A. L.; Berkdemir, A.; Wang, B.; Lv, R.; López-Urías, F.; Crespi, V. H.; Terrones, H.; Terrones, M. Extraordinary Room-Temperature Photoluminescence in WS2 Triangular Monolayers. *Nano Lett.*, in press. DOI: 10.1021/nl3026357.
2. Novoselov, K. S.; Jiang, D.; Schedin, F.; Booth, T. J.; Khotkevich, V. V.; Morozov, S. V.; Geim, A. K. Two-Dimensional Atomic Crystals. *Proc. Natl. Acad. Sci. U.S.A.* **2005**, *102*, 10451–10453.
3. Mak, K. F.; Lee, C.; Hone, J.; Shan, J.; Heinz, T. F. Atomically Thin MoS_2: A New Direct-Gap Semiconductor. *Phys. Rev. Lett.* **2010**, 105.
4. Zhan, Y. J.; Liu, Z.; Najmaei, S.; Ajayan, P. M.; Lou, J. Large-Area Vapor-Phase Growth and Characterization of MoS_2 Atomic Layers on a SiO_2 Substrate. *Small* **2012**, *8*, 966–971.
5. Splendiani, A.; Sun, L.; Zhang, Y. B.; Li, T. S.; Kim, J.; Chim, C. Y.; Galli, G.; Wang, F. Emerging Photoluminescence in Monolayer MoS_2. *Nano Lett.* **2010**, *10*, 1271–1275.
6. Eda, G.; Yamaguchi, H.; Voiry, D.; Fujita, T.; Chen, M. W.; Chhowalla, M. Photoluminescence from Chemically Exfoliated MoS_2. *Nano Lett.* **2011**, *11*, 5111–5116.
7. Coleman, J. N.; Lotya, M.; O'Neill, A.; Bergin, S. D.; King, P. J.; Khan, U.; Young, K.; Gaucher, A.; De, S.; Smith, R. J.; et al. Two-Dimensional Nanosheets Produced by Liquid Exfoliation of Layered Materials. *Science* **2011**, *331*, 568–571.
8. Lauritsen, J. V.; Kibsgaard, J.; Helveg, S.; Topsoe, H.; Clausen, B. S.; Laegsgaard, E.; Besenbacher, F. Size-Dependent Structure of MoS_2 Nanocrystals. *Nat. Nanotechnol.* **2007**, *2*, 53–58.
9. Wang, Q. H.; Kalantar-Zadeh, K.; Kis, A.; Coleman, J. N.; Strano, M. S. Electronics and Optoelectronics of Two-Dimensional Transition Metal Dichalcogenides. *Nat. Nanotechnol.* **2012**, *7*, 699–712.
10. Matte, H. S. S. R.; Gomathi, A.; Manna, A. K.; Late, D. J.; Datta, R.; Pati, S. K.; Rao, C. N. R. MoS_2 and WS_2 Analogues of Graphene. *Angew. Chem., Int. Ed.* **2010**, *49*, 4059–4062.
11. Butler, S. Z.; Hollen, S. M.; Cao, L.; Cui, Y.; Gupta, J. A.; Gutiérrez, H. R.; Heinz, T. F.; Hong, S. S.; Huang, J.; Ismach, A. F.; et al. Progress, Challenges, and Opportunities in Two-Dimensional Materials beyond Graphene. *ACS Nano* **2013**, *7*, 2898−2926.
12. Chhowalla, M.; Shin, H. S.; Eda, G.; Li, L.; Loh, K. P.; Zhang, H. The Chemistry of Two-Dimensional Layered Transition Metal Dichalcogenide Nanosheets. *Nat. Chem.* **2013**, *5*, 263–275.
13. Geim, A. K.; Novoselov, K. S. The Rise of Graphene. *Nat. Mater.* **2007**, *6*, 183–191.
14. Jin, C. H.; Lin, F.; Suenaga, K.; Iijima, S. Fabrication of a Freestanding Boron Nitride Single Layer and Its Defect Assignments. *Phys. Rev. Lett.* **2009**, 102.
15. Ci, L.; Song, L.; Jin, C. H.; Jariwala, D.; Wu, D. X.; Li, Y. J.; Srivastava, A.; Wang, Z. F.; Storr, K.; Balicas, L.; *et al.* Atomic Layers of Hybridized Boron Nitride and Graphene Domains. *Nat. Mater.* **2010**, *9*, 430–435.
16. Zeng, H. L.; Dai, J. F.; Yao, W.; Xiao, D.; Cui, X. D. Valley Polarization in MoS_2 Monolayers by Optical Pumping. *Nat. Nanotechnol.* **2012**, *7*, 490–493.
17. Mak, K. F.; He, K. L.; Shan, J.; Heinz, T. F. Control of Valley Polarization in Monolayer MoS_2 by Optical Helicity. *Nat. Nanotechnol.* **2012**, *7*, 494–498.
18. Schutte, W. J.; Deboer, J. L.; Jellinek, F. Crystal-Structures of Tungsten Disulfide and Diselenide. *J. Solid State Chem.* **1987**, *70*, 207–209.
19. Divigalpitiya, W. M. R.; Frindt, R. F.; Morrison, S. R. Inclusion Systems of Organic-Molecules in Restacked Single-Layer Molybdenum-Disulfide. *Science* **1989**, *246*, 369–371.
20. Lee, Y. H.; Zhang, X. Q.; Zhang, W. J.; Chang, M. T.; Lin, C. T.; Chang, K. D.; Yu, Y. C.; Wang, J. T. W.; Chang, C. S.; Li, L. J. *et al.* Synthesis of Large-Area MoS_2 Atomic Layers with Chemical Vapor Deposition. *Adv. Mater.* **2012**, *24*, 2320–2325.
21. van der Zande, A. M.; Huang, P. Y.; Chenet, D. A.; Berkelbach, T. C.; You, Y.; Lee, G. H.; Heinz, T. F.; Reichman, D. R.; Muller, D. A.; Hone, J. C.; Grains and Grain Boundaries in Highly Crystalline Monolayer Molybdenum Disulfide. *Nat. Mater.*, in press. DOI: 10.1038/nmat3633.
22. Najmaei, S.; Liu, Z.; Zhou, W.; Zou, X.; Shi, G.; Lei, S.; Yakobson, B. I.; Idrobo, J. C.; Ajayan, P. M.; Lou, J.; Vapor Phase Growth and Grain Boundary Structure of Molybdenum Disulfide Atomic Layers. *Nat. Mater.*, in press. Preprint at http://arxiv.org/abs/1301.2812
23. Matte, H. S. S. R.; Maitra, U.; Kumar, P.; Rao, B. G.; Pramoda, K.; Rao, C. N. R. Synthesis, Characterization, and Properties of Few-Layer Metal Dichalcogenides and Their Nanocomposites with Noble Metal Particles, Polyaniline, and Reduced Graphene Oxide. *Z. Anorg. Allg. Chem.* **2012**, *638*, 2617–2624.
24. Radisavljevic, B.; Radenovic, A.; Brivio, J.; Giacometti, V.; Kis, A. Single-Layer MoS_2 Transistors. *Nat. Nanotechnol.* **2011**, *6*, 147–150.
25. Yin, Z. Y.; Li, H.; Li, H.; Jiang, L.; Shi, Y. M.; Sun, Y. H.; Lu, G.; Zhang, Q.; Chen, X. D.; Zhang, H. Single-Layer MoS_2 Phototransistors. *ACS Nano* **2012**, *6*, 74–80.
26. Bertolazzi, S.; Brivio, J.; Kis, A. Stretching and Breaking of Ultrathin MoS_2. *ACS Nano* **2011**, *5*, 9703–9709.
27. Berkdemir, A.; Gutiérrez, H. R.; Botello-Méndez, A. R.; Perea-López, N.; Elías, A. L.; Chen-Ing Chia, C.-I.; Wang, B.; Crespi, V. H.; López-Urías, F.; Charlier, J.-C.; *et al.* Identification of Individual and Few Layers of WS_2 Using Raman Spectroscopy. *Sci. Rep.* **2013**, *3*, 1755.
28. Ferrari, A. C.; Meyer, J. C.; Scardaci, V.; Casiraghi, C.; Lazzeri, M.; Mauri, F.; Piscanec, S.; Jiang, D.; Novoselov, K. S.; Roth, S.; *et al.* Raman Spectrum of Graphene and Graphene Layers. *Phys. Rev. Lett.* **2006**, *97*, 187401.
29. Gupta, A.; Chen, G.; Joshi, P.; Tadigadapa, S.; Eklund, P. C. Raman Scattering from High-Frequency Phonons in Supported n-Graphene Layer Films. *Nano Lett.* **2006**, *6*, 2667–2673.
30. Yoon, D.; Moon, H.; Cheong, H.; Choi, J. S.; Choi, J. A.; Park, B. H. Variations in the Raman Spectrum as a Function of the Number of Graphene Layers. *J. Korean Phys. Soc.* **2009**, *55*, 1299–1303.
31. Gorbachev, R. V.; Riaz, I.; Nair, R. R.; Jalil, R.; Britnell, L.; Belle, B. D.; Hill, E. W.; Novoselov, K. S.; Watanabe, K.; Taniguchi, T.; Blake, P.; *et al.* Hunting for Monolayer Boron Nitride: Optical and Raman Signatures. *Small* **2011**, *7*, 465–468.
32. Lee, C.; Yan, H.; Brus, L. E.; Heinz, T. F.; Hone, J.; Ryu, S. Anomalous Lattice Vibrations of Single- and Few-Layer MoS_2. *ACS Nano* **2010**, *4*, 2695–2700.
33. Li, H.; Zhang, Q.; Yap, C. C. R.; Tay, B. K.; Edwin, T. H. T.; Olivier, A.; Baillargeat, D. From Bulk to Monolayer MoS_2: Evolution of Raman Scattering. *Adv. Funct. Mater.* **2012**, *22*, 1385–1390.
34. Molina-Sanchez, A.; Wirtz, L. Phonons in Single-Layer and Few-Layer MoS_2 and WS_2. *Phys. Rev. B.: Condens. Matter Mater. Phys.* **2011**, 84.
35. Najmaei, S.; Liu, Z.; Ajayan, P. M.; Lou, J. Thermal Effects on the Characteristic Raman Spectrum of Molybdenum

Disulfide (MoS_2) of Varying Thicknesses. *Appl. Phys. Lett.* **2012**, 100.
36. Frey, G. L.; Tenne, R.; Matthews, M. J.; Dresselhaus, M. S.; Dresselhaus, G. Optical Properties of MS_2 (M = Mo, W) Inorganic Fullerene-like and Nanotube Material Optical Absorption and Resonance Raman Measurements. *J. Mater. Res.* **1998**, *13*, 2412–2417.
37. Stacy, A. M.; Hodul, D. T. Raman-Spectra of Ivb and Vib Transition-Metal Disulfides Using Laser Energies near the Absorption Edges. *J. Phys. Chem. Solids* **1985**, *46*, 405–409.
38. Sourisseau, C.; Cruege, F.; Fouassier, M.; Alba, M. 2nd-Order Raman Effects, Inelastic Neutron-Scattering and Lattice-Dynamics in 2h-WS_2. *Chem. Phys.* **1991**, *150*, 281–293.
39. Ma, Y. D.; Dai, Y.; Guo, M.; Niu, C. W.; Lu, J. B.; Huang, B. B. Electronic and Magnetic Properties of Perfect, Vacancy-Doped, and Nonmetal Adsorbed $MoSe_2$, $MoTe_2$ and WS_2 Monolayers. *Phys. Chem. Chem. Phys.* **2011**, *13*, 15546–15553.
40. Ballif, C.; Regula, M.; Schmid, P. E.; Remskar, M.; Sanjines, R.; Levy, F. Preparation and Characterization of Highly Oriented, Photoconducting WS_2 Thin Films. *Appl. Phys. A: Mater. Sci. Process.* **1996**, *62*, 543–546.
41. Frey, G. L.; Elani, S.; Homyonfer, M.; Feldman, Y.; Tenne, R. Optical-Absorption Spectra of Inorganic Fullerenelike MS_2 (M = Mo, W). *Phys. Rev. B.: Condens. Matter Mater. Phys.* **1998**, *57*, 6666–6671.
42. Dumcenco, D. O.; Kobayashi, H.; Liu, Z.; Huang, Y. S.; Suenaga, K. Visualization and Quantification of Transition Metal Atomic Mixing in $Mo_{1-x}W_xS_2$ Single Layers. *Nat. Commun.* **2013**, *4*, 1351.
43. Komsa, H. P.; Krasheninnikov, A. V. Two-Dimensional Transition Metal Dichalcogenide Alloys: Stability and Electronic Properties. *J. Phys. Chem. Lett.* **2012**, *3*, 3652–3656.